The chemical basis of serine palmitoyltransferase inhibition by myriocin

Cite as:
Wadsworth, J. M., Clarke, D. J., McMahon, S. A., Lowther, J. P., Beattie, A. E., Langridge-Smith, P. R. R., Broughton, H. B., Dunn, T. M., Naismith, J. H., & Campopiano, D. J. (2013). The chemical basis of serine palmitoyltransferase inhibition by myriocin. *Journal of the American Chemical Society*, 135(38), 14276-85.

Manuscript received: 14/06/2013; Accepted: 19/08/2013; Article published: 11/09/2013

The chemical basis of serine palmitoyltransferase inhibition by myriocin**

John M. Wadsworth,[1,#] David J. Clarke,[1,#] Stephen A. McMahon,[2] Jonathan P. Lowther,[1] Ashley E. Beattie,[2] Pat Langridge-Smith,[2] Howard Broughton,[3] Teresa M. Dunn,[4] James H. Naismith[2] and Dominic J. Campopiano[1,*]

[1]EaStCHEM, School of Chemistry, Joseph Black Building, University of Edinburgh, West Mains Road, Edinburgh, EH9 3JJ, UK.

[2]Biomedical Sciences Research Complex, The University, St Andrews, KY16 9ST, UK.

[3]Molecular Modelling Laboratory, Centro de Investigación Lilly, S.A., Avda. de la Industria, 30. 28108-Alcobendas. Madrid. Spain.

[4]Department of Biochemistry and Molecular Biology, Uniformed Services University of the Health Sciences, Bethesda, Maryland, USA.

[*]Corresponding author; dominic.campopiano@ed.ac.uk

[**]We wish to thank the BBSRC for awarding grants to D.J.C. (BB/I013687/1) and J.H.N. (BB/F009739/1) that support D.J.Cla/J.P.L. and S.A.McM. respectively. J.M.W. is supported by a joint PhD studentship between the University of Edinburgh and Lily pharmaceuticals. A.E.B. is supported by a joint PhD studentship between the University of Edinburgh and The Derek Stewart Charitable Trust. The collaboration between D.J.C. and T.M.D. is supported by BBSRC grant (BB/G53045X/1).

Supporting information:
Supporting material is available free of charge via the Internet at http://pubs.acs.org

Author contributions:
[#] These authors contributed equally.

Abstract

Sphingolipids (SLs) are essential components of cellular membranes formed from the condensation of L-serine and a long-chain acyl thioester. This first step is catalysed by the pyridoxal 5□-phosphate (PLP)-dependent enzyme serine palmitoyltransferase (SPT) which is a promising therapeutic target. The fungal natural product myriocin is a potent inhibitor of SPT and is widely-used to block SL biosynthesis despite a lack of a detailed understanding of its molecular mechanism. By combining spectroscopy, mass spectrometry, x-ray crystallography and kinetics we have characterised the molecular details of SPT inhibition by myriocin. Myriocin initially forms an external aldimine with PLP at the active site and a structure of the resulting co-complex explains its nanomolar affinity for the enzyme. This co-complex then catalytically degrades via an unexpected 'retro-aldol like' cleavage mechanism to a C18 aldehyde which in turn acts as a suicide inhibitor of SPT by covalent modification of the essential catalytic lysine. This surprising dual mechanism of inhibition rationalises the extraordinary potency and longevity of myriocin inhibition.

Keywords

Serine palmitoyltransferase, pyridoxal-5'-phosphate, sphingolipid, natural product, myriocin, suicide inhibition, alpha-oxoamine synthase.

Abbreviations

SPT, serine palmitoyltransferase: PLP, pyridoxal-5'-phosphate: AOS, alpha-oxoamine synthase: KDS, 3-keto dihydrosphingosine: CoA, coenzyme A: DTNB, 5,5'-dithio-bis(2-nitrobenzoic acid): ESI, Electrospray ionisation; LC-MS, Liquid chromatography mass spectrometry: FT-ICR, Fourier transform ion cyclotron resonance.

Graphical abstract

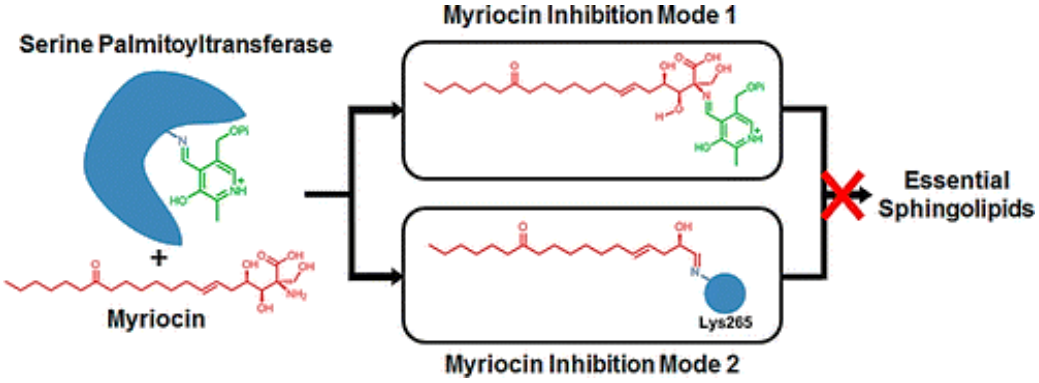

Introduction

Sphingolipids (SLs) are a large sub class of lipids which are defined by the presence of an amino alcohol functionality of sphingosine (or similar).[1] SLs have been implicated in a wide range of cellular functions and linked to diseases such as diabetes, Alzheimer's and asthma.[2] Controlling their production is under intense investigation as a new strategy in pharmaceutical therapy. For example, the drug fingolimod, which mimics sphingosine, is used for the treatment of multiple sclerosis and is the first SL-derived therapeutic agent used in the clinic.[3] Serine palmitoyltransferase (SPT, EC 2.3.1.50) is a member of the α-oxoamine synthase (AOS) family of PLP-dependent enzymes along with 8-amino-7-oxononanoate synthase (AONS)[4], 2-amino-3-ketobutyrate ligase (KBL)[5], 5-aminolevulinate synthase (ALAS)[6] and cholera quorum-sensing autoinducer synthase CqsA[7]. SPT catalyses the first and rate-determining step in the SL biosynthetic pathway, the decarboxylative, Claisen-like condensation between L-serine (**2**) and an acyl-CoA thioester (**4**) to generate the long-chain base intermediate, 3-ketodihydrosphingosine (KDS, **9, Figure 1**). The postulated mechanism involves a number of intermediates including a PLP-bound internal aldimine (**1,** also known as the holo-form), a PLP-L-serine external aldimine (**3**), a quinonoid or masked carbanion (**6**) and a key □-keto acid condensation intermediate (**8**).[8]

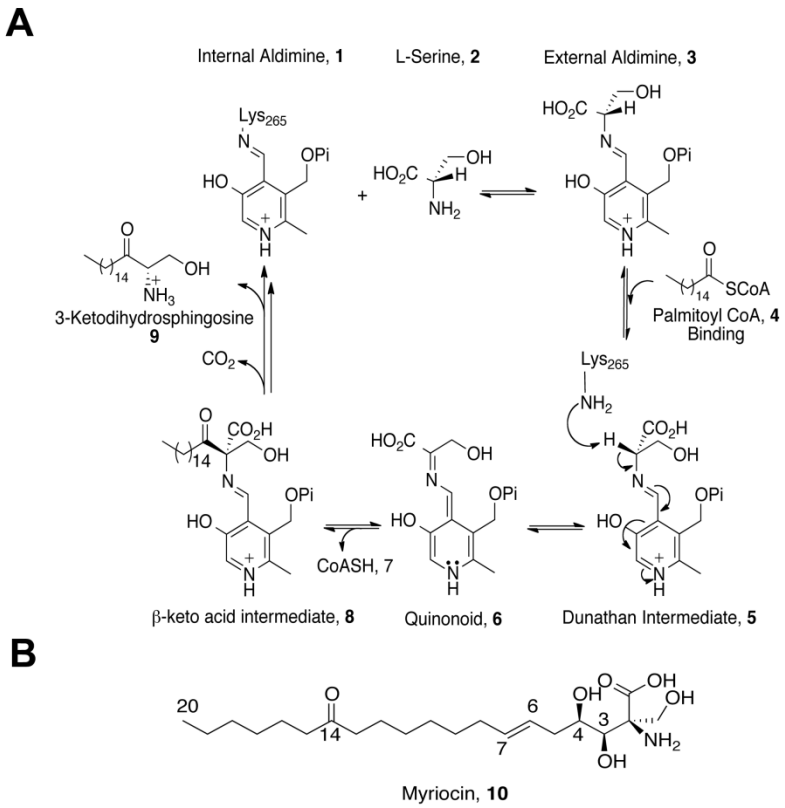

Figure 1. The PLP-dependant catalytic mechanism of SPT. (A) The internal aldimine, **1** (holo-SPT) is displaced by L-serine, **2**, to form the external aldimine, **3**. Binding of the second substrate, palmitoyl-CoA, **4**, causes conformational change to give the Dunathan intermediate, **5**. This conformation allows deprotonation of Cα hydrogen by Lys265, forming the quinonoid, **6**. This is followed by nucleophilic attack on the

palmitoyl-CoA thioester from Cα, releasing CoASH, **7**, forming the β-keto acid intermediate, **8**. This intermediate undergoes decarboxylation, before release of the product 3-ketodihydrosphingosine (KDS), **9**, and regeneration of the internal aldimine, **1**. (B) The natural product SPT inhibitor myriocin, **10**.

Over 160 PLP-dependent enzymes have been characterised[9] and mechanistic studies of non-specific PLP inhibitors such as cycloserine, penicillamine, and β-chloro-alanine[10] have greatly enhanced the understanding of PLP chemistry as well as highlighting the diversity of reactions that use this organic cofactor as a catalyst. Consequently, PLP-dependent enzymes are now recognised as attractive drug targets.[11] Despite the importance of both PLP enzymes in general and SPT in particular, only a small number of SPT-specific inhibitors have been discovered, all of which are natural products - sphingofungins, viridiofungin A, lipoxamycin and myriocin (**10**, **Figure 1B**).[12] Myriocin [(2*S*,3*R*,4*R*,6*E*)-2-Amino-3,4-dihydroxy-2-(hydroxymethyl)-14-oxo-6-eicosenoic acid], also known as thermozymocidin and ISP-1, was first discovered in 1972 by two independent groups[13] from the thermophilic moulds *Myriococcum albomyces* and *Mycelia sterilia* and both found the natural product to be a potent antifungal agent. It was re-isolated from the fungus *Isaria sinclairii* in 1994 and shown to be a potent immunosuppressant.[14] Kawasaki and colleagues[12d] determined an IC_{50} value of 15 nM, using the mouse cytotoxic T-cell line, CTLL-2 as a model for myriocin-dependent inhibition of cell growth and elimination of ceramide production. Since growth was restored by the addition of sphingosine, it suggested that SPT was the primary target of myriocin. In 1999 Schreiber and colleagues used a myriocin-like affinity resin to identify the two subunits of murine SPT (SPT1 and SPT2 encoded by the genes, *lcb1* and *lcb2* respectively) as the primary targets of the natural product myriocin.[15]

Myriocin remains the most valuable and widely used chemical probe in SL research; for example recent studies using the natural product in whole eukaryotic cells and cell extracts have revealed unexpected structural complexity in the membrane-bound SPTs from higher organisms.[2c, 16] Despite its use, the molecular basis of myriocin inhibition of SPT is largely unknown. To shed light on the chemistry of this important enzyme:inhibitor complex we have used a soluble, recombinant form of the enzyme from the SL-producing bacterium *Sphingomonas paucimobilis* which has proven an informative model system. Here we present a detailed chemical analysis of the SPT:myriocin inhibition mechanism including a structural description of the covalent PLP:external aldimine of myriocin. We also reveal an unexpected, enzyme-catalysed myriocin degradation mechanism that generates a second species which acts as a suicide inhibitor of its enzyme target; thus we propose that myriocin acts as a novel dual-mode inhibitor of SPT.

Experimental section

Chemicals and Molecular Biology Tools. Plasmids and competent cells were purchased from Novagen. All buffers and reagents were from Sigma. Palmitoyl-CoA was purchased from Avanti Lipids, and myriocin was purchased from Sigma.

Gene cloning and mutagenesis. The *S. paucimobilis* SPT used in this study is in vector pET28a and contains a six histidine tag at the N-terminus. This generates an SPT of 441 amino acids with a short extension at the N-terminus containing the His tag and a 12 amino acid linker. The K265A mutant was made using the Liu mutagenesis protocol[17] with the following primers:

5'-gtcggcactttctct**gcg**tctgttggaactgttggc-3' (Forward),

5'-acccgccaacagttccaacaga**cgc**agagaaagtgccgac-3' (Reverse).

The bases mutated are shown in bold and the isolated SPT K265A clone was verified by DNA sequencing. Mass spectrometry analysis of both wild type and K265A mutant SPTs showed the proteins to be intact with only the N-terminal methionine removed. To avoid confusion and allow comparison with previous data we number the N-terminally-tagged SPT using the same sequence as before.[8] Key active site residues are His159, Asp231, His234, and Lys265.

Expression and purification of SPT WT and SPT K265A mutant. Expression and purification of the WT protein has been reported previously.[8] A single colony of pET-28a SPT BL21 (DE3) (or SPT K265A mutant) was used to inoculate 250 ml of LB media with kanamycin (30 μg $mL^{-1)}$ and grown overnight to saturation. This culture was diluted 1:100 in fresh LB / kanamycin and grown to an OD_{600} of 0.6 before expression was induced with 0.1 mM Isopropyl β-D-1-thiogalactopyranoside (IPTG). Protein expression continued for 5 hours at 30 °C, 200 rpm. Harvested cells where re-suspended in lysis buffer 20 mM KPhos, pH 7.5, 150 mM NaCl, 10 mM imidazole, 25 μM PLP and complete protease inhibitor cocktail (Roche) and lysed by sonication (Soniprep 150, 15 cycles of 30 sec on followed by 30 sec off) on ice. The resulting lysate was centrifuged for 30 mins at 47000 g. The supernatant was incubated with Ni resin (Ni-NTA Superflow, Qiagen) for 1 hour at 4 °C. The resin was removed, washed and the protein eluted in lysis buffer supplemented with 300 mM imidazole. Imidazole was removed by dialysis of the protein into 20 mM KPhos, pH 7.5,150 mM NaCl, 25 μM PLP before a final gel filtration purification step using a Superdex S200 column (GE Healthcare) equilibrated and eluted with 20 mM Tris, pH 7.5,150 mM NaCl, 25 μM PLP buffer. The purity of the eluted protein was checked by SDS PAGE and the protein identity confirmed by mass spectrometry.

UV-vis Spectroscopic Measurements. All UV-visible spectra were recorded on a Cary 50 UV-visible spectrophotometer (Varian) and analyzed using Cary WinUV software (Varian). Immediately prior to enzymatic assays, SPT was converted to the holo-form by dialysis against freshly-prepared 20 mM KPhos (pH 7.5) containing 150 mM NaCl and 25 μM PLP for 1 h at 4 °C. Excess PLP was removed by passing the protein through a PD-10 (Sephadex G-25M) desalting column (GE Healthcare) before concentration to 40 μM using a VivaSpin 30 kDa cut-off concentration filter. For UV-visible analysis, the concentration of recombinant SPT was 40 μM, and the spectrophotometer was blanked with 20 mM potassium phosphate (pH 7.5) containing 150 mM NaCl. The spectrophotometer was maintained at a constant temperature throughout all time-dependant assays using a Cary PCB-150 single cell Peltier.

SPT Activity Assay. SPT activity was measured using a previously published method that uses a continuous spectrophotometric assay to monitor the release of CoASH from acyl-CoA substrates and reaction with 5,5′-dithiobis-2-nitrobenzoic acid (DTNB).[8b] Assays were performed on a 250 μL scale on a 96-well format in a Biotek Synergy HT plate reader. The enzyme was incubated with L-serine and myriocin in a buffered solution containing DTNB, and the assay was started by the addition of the second substrate, palmitoyl-CoA. The CoASH thiol product was monitored by observation of the TNB^- anion at 412 nm (ε_{max} = 14,150 M^{-1} cm^{-1}) for 45 minutes. A typical experiment contained 0.2 μM SPT, 20 mM L-serine, 250 μM palmitoyl-CoA, and 0.2 mM DTNB in 100 mM HEPES, pH 8.0. Kinetic constants were calculated using GraphPad Prism 6 software. K_m and competition experiments where performed and calculated using Michaelis-Menten kinetics.

Inhibition Studies. Due to the tight binding nature of myriocin, it was necessary to calculate inhibition kinetics using the regimen described by Williams and Morrison.[18] The Michaelis-Menten equation can not be used as the assumption that the free inhibitor concentration is equal to the total inhibitor concentration is not valid; instead the K_i is calculated using the quadratic Morrison equation. The K_m for L-serine was calculated from rates measured with increasing concentrations of L-serine (0.1-40 mM) while maintaining the palmitoyl-CoA concentration at 250 μM in excess of its K_m (35 μM). Similarly, the K_m for palmitoyl-CoA was calculated from rates measured with increasing concentrations of palmitoyl-CoA (2.5-1500 μM) and excess L-serine (20 mM).

In order to determine the type of inhibition between SPT and myriocin, IC_{50} values for the inhibitor were determined in the presence of a number of different substrate concentrations (both L-serine and palmitoyl-CoA). During these experiments the enzyme concentration remained fixed at 200 nM. In order to ensure solubility of myriocin in the assay mixture, myriocin was dissolved in DMSO then diluted to its final desired concentration with the DMSO concentration at less than or equal to 1%. For the experiments varying palmitoyl-CoA concentration it was necessary to add L-ser and palmitoyl-CoA prior to addition of myriocin. The resulting IC_{50} values were plotted against substrate concentrations in a manner described by Cha, Williams and Morrison [19]. All kinetic experiments were performed in triplicate.

To determine the reversibility of inhibition, 40 μM SPT was treated with 200 μM myriocin and incubated for either 10 minutes or 16 hours at 25 °C. Excess inhibitor was then removed by extensive dialysis against 20 mM KPhos, 150 mM NaCl, pH 7.5 with 25 μM fresh PLP. Aliquots were then removed at specific timepoints and assayed for SPT activity as above.

Mass Spectrometry. All mass spectra were acquired using a 12 Telsa SolariX FT-ICR mass spectrometer equipped with an electrospray ion source (Bruker Daltonics). LC-MS experiments were performed using an Ultimate 3000 HPLC system (Dionex).

For the detection of the PLP-myriocin aldimine (**11**) and the PLP-decarboxymyriocin aldimine (**15**), samples were prepared by incubating myriocin (200 μM) with either wildtype or K265A SPT (40 μM) at 25 °C. At

specific time points, aliquots were removed and analysed by LC-MS using a Phenomenex C18 Aeris Widepore 50 x 2.1mm column, operating at a flow rate of 150 µl/min. A gradient of 2 to 98% acetonitrile was performed over 20 minutes. In order to preserve the acid labile imine bond, no acidic modifiers were added to either mobile phase. For single ion monitoring, the mass resolving quadrupole was set to a specific *m/z*, with a 10 *m/z* window, and ions were typically accumulated for 2000 milliseconds.

For intact protein mass spectrometry, LC-MS was performed using a monolithic PS-DVB (500 µm x 50 mm) reverse-phase analytical column (Dionex). Protein (100 pmoles) was loaded onto the column (maintained at 60 °C) followed by a 10 min linear gradient from 2 to 95% acetonitrile (flow rate 20 µl/min). Mass spectra were collected every 200 ms between *m/z* 600-2500. Data analysis was performed using DataAnalysis software (Bruker Daltonics). Neutral spectra were created using Maximum Entropy deconvolution.

Peptide Mass Mapping. For peptide mass mapping, SPT (40 µM) was treated with 200 µM myriocin. Derivitization was allowed to proceed for 18 hours at 25 °C, whilst being monitored by UV-vis spectroscopy. After loss of the peak at 430 nm in the UV-vis spectrum, the sample was chemically reduced by treatment with 10 mM $NaBH_4$. Finally, this sample was treated with the protease trypsin (Promega, sequence grade) for 18 h at 37 °C at an enzyme:protein ratio of approximately 1:20 by weight. The resulting peptide mixture was analysed by LC-MS using a monolithic PS-DVB (500 µm x 50 mm) reverse-phase analytical column (Dionex). The column was maintained at 60 °C, and a linear gradient of 5-70% acetonitrile was performed over 30 minutes.

The resulting data was analysed by DataAnalysis software (Bruker Daltonics). A mass list was created using the SNAP 2.0 algorithm (Bruker Daltonics) and searched against the known primary sequence of SPT using the MS-Fit software (University of California). For data searching, error tolerances were set to 10 ppm.

Structural Biology. Protein for crystallization was concentrated to 20 mg mL^{-1} and incubated with 5 equivalents of myriocin immediately prior to crystallization trials. Crystals of K265A SPT were grown by vapour drop diffusion at 20 °C over the course of two weeks and are readily reproducible. The optimum growth conditions are 32% PEG MME 2000, 0.1 M HEPES pH 7.5 and a protein:precipitant ratio of 1:1. Prior to data collection the crystals were cryo-cooled in mother liquor doped with 20% glycerol. Data were collected at Beamline I04-1 at the Diamond synchrotron light source, Oxfordshire, England and processed in an automated manner using Xia2.[20] The structure was solved by molecular replacement using PHASER[21] and PDB code 2JG2 as a model. The myriocin dictionary was created using PRODRG.[22] The model was refined using REFMAC5[23] with TLS. COOT[24] was used for manual manipulation of the structure and model quality was assessed throughout with MOLPROBITY[25]. Data collection and refinement statistics can be found in supplementary Table 2.

Accession codes. Protein Data Bank (PDB): The crystallographic data for the SPT -PLP:decarboxymyriocin structure is deposited under accession code 4BMK.

Results

Formation of a PLP-myriocin aldimine in wild-type SPT. Holo-SPT (**1**) displays a characteristic UV-vis spectrum for a PLP-containing protein with absorption maxima at 333 nm and 420 nm (**Figure 2A**), corresponding to the equilibrium between the ketoenamine and enolimine forms of PLP.[8b] Addition of fivefold molar excess of myriocin to holo-SPT led to an immediate increased absorbance with a maximum at 430 nm and loss of the 333 nm peak as previously observed by Ikushiro *et al*.[12b] Hanada *et al.* proposed that this species corresponds to a PLP-myriocin aldimine (**11**) formed as a result of transimination (**Figure 2B**) that acts as a stable mimic of the β-keto acid intermediate (**8**) in the SPT mechanism (**Figure 1**).[26] LC ESI-MS analysis detects a species of monoisotopic mass 631.30153 Da consistent with the PLP-myriocin aldimine (**11**) (Predicted monoisotopic mass 631.29902 Da; $[(C_{29}H_{47}N_2O_{11}P)+H]^+$) (**Figure 2C**). Attempts to trap the reduced form of (**11**) using $NaBH_4$ were unsuccessful.

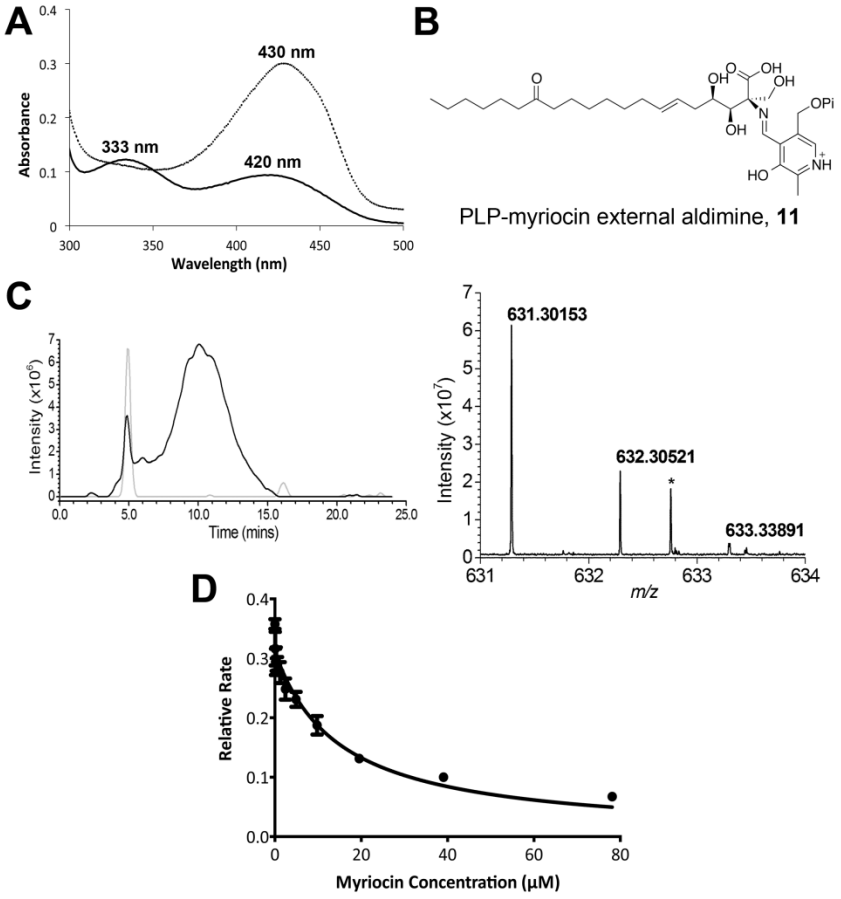

Figure 2. SPT inhibition occurs via formation of a PLP-myriocin aldimine. (A) UV-Vis spectrum of 40 μM SPT before (solid line) and after 200 μM myriocin addition (dotted line). (B) The proposed structure of the inhibitory complex - a PLP-myriocin aldimine, **11**. (C) Detection of the PLP-myriocin aldimine by LC-MS. *Top*, Extracted Ion Chromatogram at *m/z* 631. *Bottom*, high resolution mass spectrum of the PLP-myriocin

aldimine, obtained by summing the spectra between t = 8-12 minutes. ($[M+H]^+$ $C_{29}H_{48}N_2O_{11}P$; predicted *m/z* 631.29902; observed error 4.0ppm). * denotes a contaminant. (D) Inhibition of SPT by myriocin, data fitted using the Morrison equation. The K_i obtained for the PLP-myriocin aldimine is 967 ± 98 nM.

Using the method by Cha,[19a] IC_{50} values for the inhibitor were determined at fixed enzyme concentrations whilst systematically varying each substrate concentration. IC_{50} values increase linearly with varying L-serine and palmitoyl-CoA concentration, establishing myriocin as a competitive inhibitor for both L-serine and palmitoyl-CoA substrates (**Supplementary Figure 1**). The Morrison equation[19b], yields a K_i for myriocin of 967 ± 98 nM (**Figure 2D**).

The PLP-myriocin inhibitory complex undergoes slow catalytic degradation. The PLP-myriocin aldimine (**11**) at 25 ^oC was stable for 90 minutes before a slow spectral transition took place over 16 hours (decrease at 430 nm and a concomitant increase at 331 and 400 nm) (**Figure 3A**); indicating conversion of **11** to a previously unseen PLP aldimine. To our surprise the new species remained catalytically compromised, indicating the new PLP aldimine is also inhibitory. Immediately after addition of myriocin only 7.7% of enzyme activity remains (as expected); however after complete conversion (judged by no further change in the UV-vis spectrum) activity remained low at 10.1% relative to the starting value (**Figure 3B**). Lowering the temperature to 4 °C arrested the decomposition of the PLP-myriocin aldimine (**Supplementary Figure 2**). Interestingly, a catalytically-inactive mutant, SPT K265A, displayed two peaks with λ_{max} values of 326 nm and 402 nm, consistent with PLP bound non-covalently as the aldehyde (**Figure 3C**). Upon incubation with five-fold molar excess of myriocin we observed a large shift to a single absorbance maximum at 425 nm similar to that observed in the wild type SPT. In contrast to the wild-type incubation this spectrum remained unchanged over 16 hrs at 25 °C indicating a stable PLP-myriocin external aldimine. Taken together, these intriguing observations suggest that the initial SPT:PLP-myriocin inhibitor complex breaks down to form a second species that also inhibits SPT.

To test the reversibility of inhibition we first generated the SPT:PLP-myriocin complex by incubation of SPT with the inhibitor for 10 minutes and 16 hrs at 25 °C. After this incubation period the temperature was lowered to 4 °C to stop further conversion and extensive dialysis against buffer containing 25 □M fresh PLP was performed for 24 hours. Aliquots were removed from the dialysate at specific time points (0, 3 and 24 hours) and assayed for SPT activity (**Figure 3D**). For the enzyme incubated with myriocin for the shorter time (10 mins), then dialysed for 3 hours, no significant activity was recovered; however, dialysis for 24 hours recovered 60% enzymatic activity (**Figure 3D**, white bars). This regain in enzymatic activity was also accompanied by a change in the UV-vis spectrum back to the internal aldimine form – i.e. λ_{max} 333 and 420 nm (data not shown). Taken together, this data from short, 10 minute incubations of SPT with myriocin is

consistent with the formation of an initial enzyme-inhibitor complex which is noncovalent in nature and reversible, albeit with a very slow off rate (k_{off}). Thus this analysis supports our assignment of the PLP-myriocin aldimine (**11**) as the initial inhibitory species. In contrast, for the enzyme preincubated with myriocin for 16 hours, no detectable regain in activity was observed after dialysis either at 3 or 24 hours (**Figure 3D**, grey bars); indicating that this second, newly-formed species acts as an irreversible inhibitor of SPT.

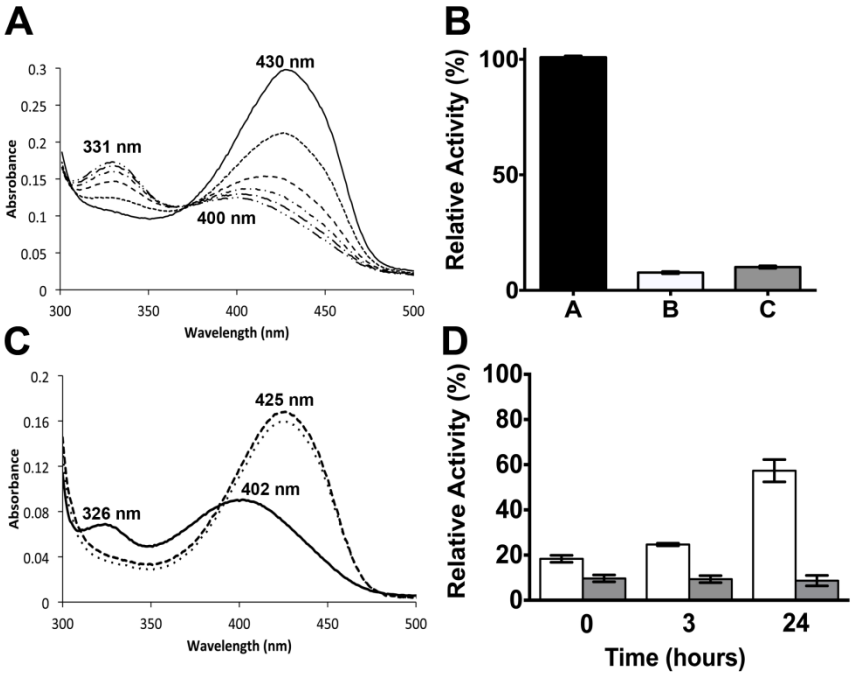

Figure 3. The PLP-myriocin aldimine undergoes SPT-catalysed degradation to form a second inhibitory species. (A) UV-vis analysis of the degradation of the PLP-myriocin external aldimine in wild-type SPT. The PLP-myriocin external aldimine (solid line) is stable for 90 minutes, before a decrease at 430 nm is observed, which is accompanied by a concomitant increase at 331 and 400 nm over 16 hours (dotted and dashed lines). (B) Relative activity of wild-type SPT after incubation with myriocin. *A*, wild type SPT activity (100%). *B*, wild-type SPT activity after 10 minutes incubation with 200 μM myriocin (7.7%). *C*, wild-type SPT activity after 16 hour incubation with 200 μM myriocin (10.1%). (C) UV-vis analysis of SPT K265A (40 μM) showed two absorbance maxima at 326 and 402 nm (solid line). Upon addition of 200 μM myriocin, an immediate shift to a single peak at 425 nm occurred (dotted line), indicating the formation of a PLP-myriocin aldimine complex. Over 16 hours this spectrum remains unchanged (dashed line), indicating that the PLP-myriocin aldimine complex is not degraded by this mutant enzyme. (D) Relative enzymatic activity after removal of inhibiting species by dialysis. SPT was inhibited with 200 μM myriocin and incubated for 10 minutes (white bars) or 16 hours (grey bars) at 25 °C before removal of myriocin by extensive dialysis. The enzymatic activity was then determined at 0 hours, 3 hours, and 24 hours after dialysis.

SPT-catalysed myriocin degradation occurs via a 'retro-aldol-like' mechanism. Our spectroscopic and kinetic observations, coupled with a detailed understanding of the mechanism of SPT and other PLP-dependant enzymes[7], allowed us to consider possible breakdown mechanisms of the SPT:PLP-myriocin complex. We postulated that a slow, "retro-aldol like" process occurs during prolonged enzyme-inhibitor incubations (**Figure 4**). To test this hypothesis we used mass spectrometry analysis to attempt the detection of the low molecular weight products of the reaction. Unfortunately, using several derivatisation methods (Girard's Reagent T; 2,4-dinitrophenylhydrazine), we were unable to capture the putative long chain octadecenal product (**12**).

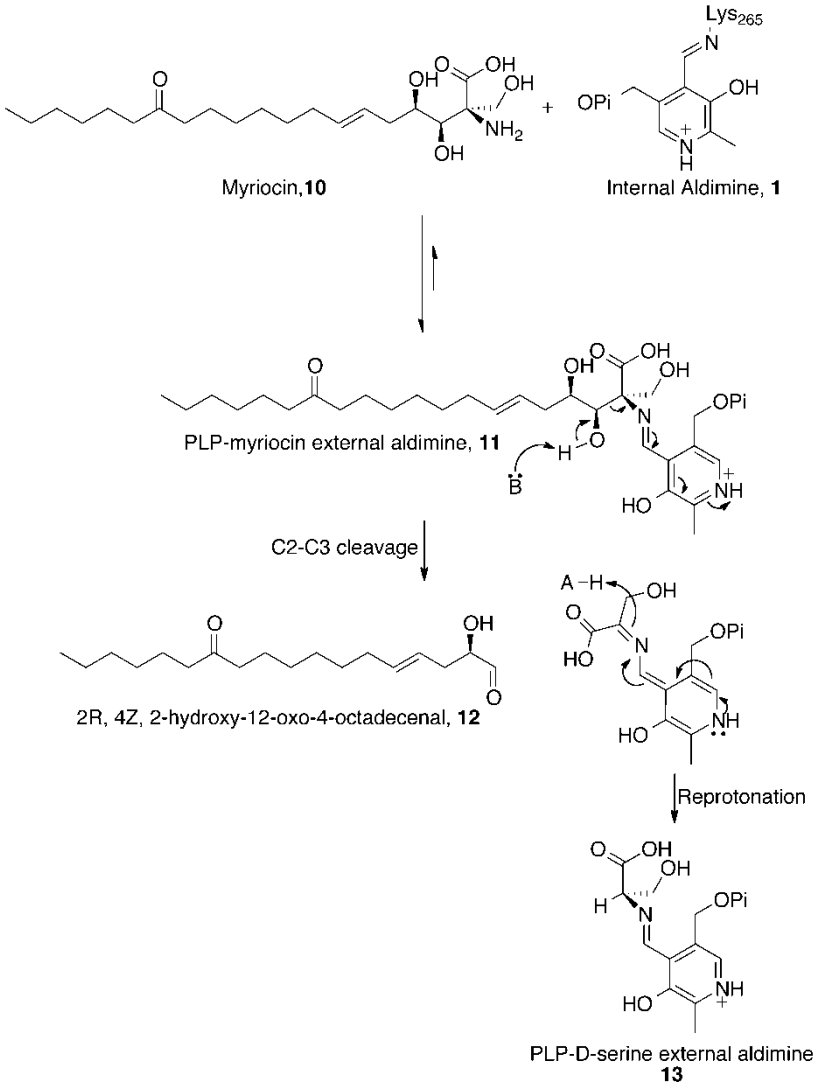

Figure 4. The proposed "retro-aldol like"mechanism for the observed degradation of the PLP-myriocin aldimine. Myriocin, **10**, undergoes fast transamination with the internal aldimine, 1, releasing Lys265 and forming the PLP-myriocin aldimine inhibitory complex, **11**. This inhibitory complex is slowly degraded by deprotonation of the myriocin C_3-hydroxyl, with C2-C3 bond cleavage and movement of electrons into the pyridine ring of PLP. This results in the formation of a 2-hydroxyl-C_{18} aldehyde species, **12**, and a PLP-D-serine aldimine, **13.**

The reason for this became clear after intact protein mass spectrometry analysis of the SPT:myriocin reaction after 16 hrs incubation at 25 °C (**Figure 5**). We detected a covalent adduct of SPT (**14**) with a mass matching that of the wild-type enzyme modified by a condensation with the predicted octadecenal (**12**) (47,509 Da, Δmass +278 Da**, Figure 5A**). This condensation product (**14**) *was* susceptible to $NaBH_4$ reduction which led to an increase in mass of the adduct by 4 Da (47,513 Da, **Supplementary Figure 3**); consistent with chemical reduction of a covalent SPT-octadecenal imine adduct as well as reduction of the ketone at position 12 of the carbon chain in (**14**). Peptide mass fingerprinting identified Lys265 as the site of modification (**Figure 5B** and **supplementary Table 1**). After trypsin digest and MS analysis, three peptide species were observed which displayed monoisotopic masses consistent (within error 4ppm) with Lys265 modified by Δmass +282.24 Da ($+C_{18}H_{34}O_2$) (**Supplementary Figure 4**). This observation of a myriocin-derived adduct at Lys265 of SPT provides convincing evidence for our proposed retro-aldol like breakdown of the PLP-myriocin aldimine to a reactive product which selectively covalently modifies an essential residue in SPT. The formation of this adduct also accounts for the irreversible nature of inhibition observed during prolonged SPT:myriocin incubations.

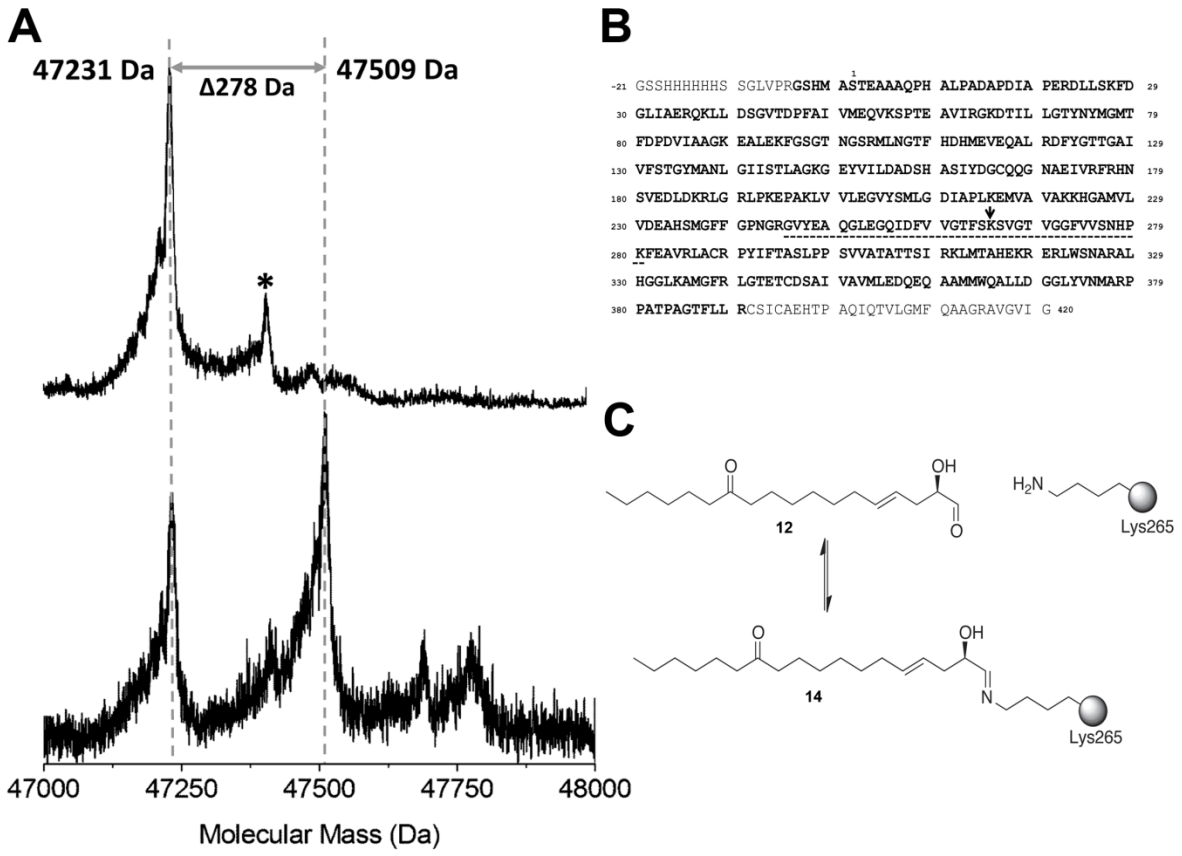

Figure 5. Mass spectrometry analysis of the myriocin-derived covalent modification of SPT. (A) Intact protein mass spectrometry of SPT (40 μM) before (*top*) and after (*bottom*) 16 hour treatment with 200 μM

myriocin at 25 °C. SPT displays an average neutral mass of 47231 Da. After myriocin treatment a prominent new species of average mass 47509 is observed (Δmass +278 Da). Minor peaks highlighted by * arise from α-*N*-gluconoylation of the His-tag. (B) Sequence coverage achieved when analysing myriocin-modified SPT enzyme. Amino acids highlighted in bold were observed in the peptide mass fingerprint (**see also supplementary Table 1**). The myriocin derived modification was isolated to a single site between Glu245 and Lys280 (underlined); this sequence contains a single internal lysine residue, Lys265 (highlighted by the arrow). (C) The myriocin-derived modification displayed a Δmass + 282.24 Da (after hydride reduction; **see also Supplementary Figure 4**), this is consistent with condensation of the C18-aldehyde (**12**) onto the amine of Lys265 forming the imine (**14**), with subsequent chemical reduction of the imine and ketone functional groups ($+C_{18}H_{34}O_2$).

Structure of a SPT K265A:PLP-myriocin external aldimine complex. We were unable to prepare crystals of the wild type SPT:PLP-myriocin aldimine complex, most likely due to aldimine degradation. However crystals of SPT K265A were obtained that diffracted to 1.6 Å resolution and contained a canonical dimer in the asymmetric unit (**Figure 6A**). The mobility/flexibility of the acyl chain prevented us from assigning a structure beyond carbon 9 of myriocin. Nevertheless difference electron density revealed a PLP-myriocin aldimine complex had formed (**Figure 6B**). The myriocin stereochemistry is retained - the *Z* configuration of the double bond at position C6 and *cis* diol geometry at positions C3 and C4. We were surprised to discover that the density indicates that myriocin had undergone loss of the carboxylate from the C2 position to form a PLP-decarboxymyriocin aldimine (**15)**. We built the model reasoning the replacement of the carboxylate with a proton (sp^3 hybridised carbon) but the resolution on its own is not sufficient to distinguish an sp^3 from an sp^2 carbon (**Figure 6B**). As had been noted previously[8b] residues from both SPT subunits are involved in PLP binding and the active site is at the dimer interface (**Figure 6C**).

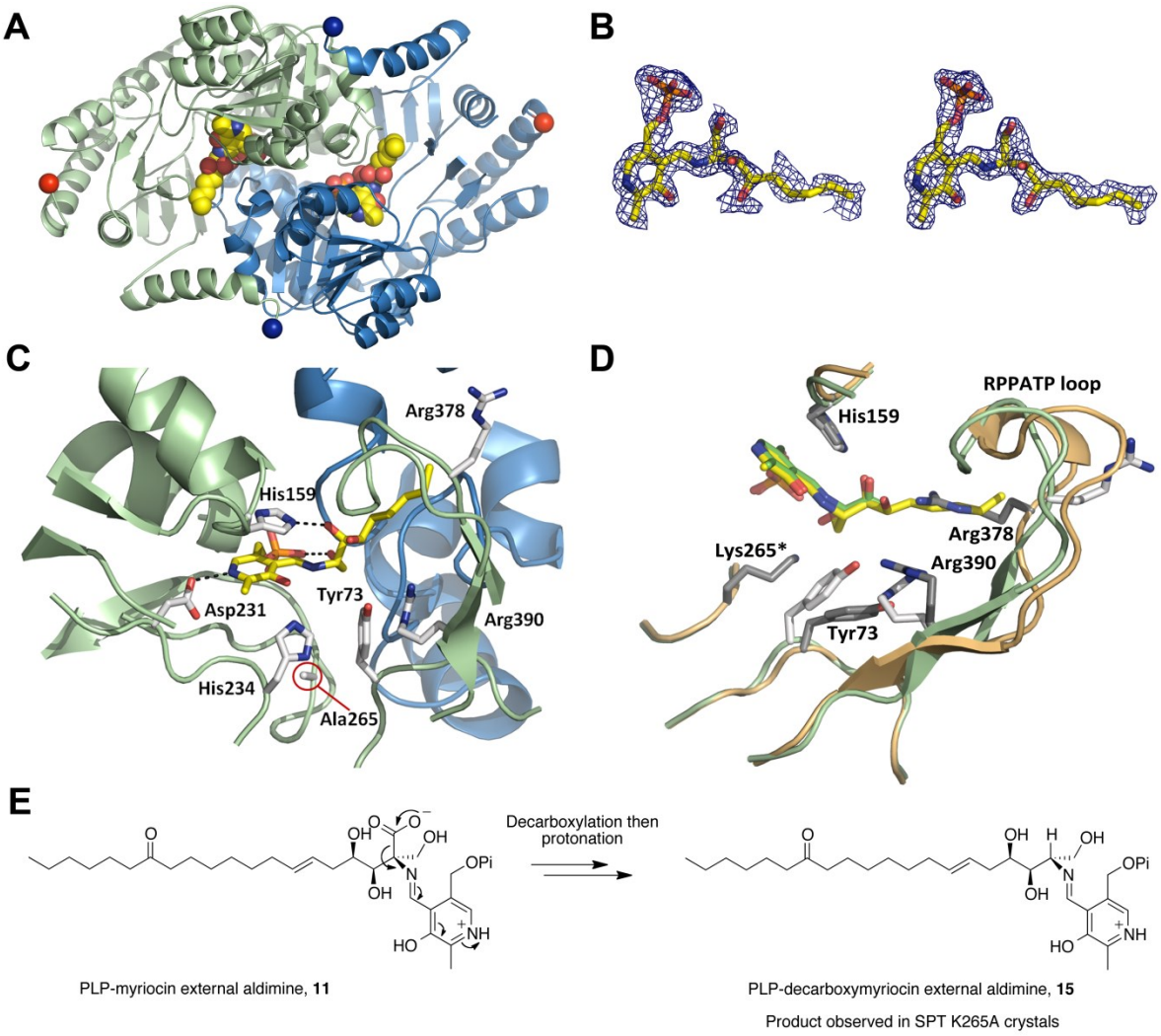

Figure 6. The structure of SPT K265A PLP-decarboxymyriocin aldimine inhibitory complex. (A) The biological SPT dimer of the decarboxylated myriocin complex. The protein is shown as a cartoon with one subunit colored pale green and the other pale blue. The PLP external aldimine of the decarboxylated myriocin (**15**) is shown in space fill with carbons colored yellow, nitrogen blue, phosphorous orange. The N terminii are marked as dark blue spheres and C-terminii as red spheres. (B) Left, The Fo-Fc map (blue chicken wire contoured at 1.8σ, carve radius 1.5Å) calculated from a model which had never contained either PLP or myriocin. Atoms are colored as figure 6A. Right, the final Fo-Fc map contoured at 0.85σ with a carve radius 1.8Å. (C) Detailed representation of the active site interactions, carbon atoms are colored yellow and shown in sticks for the PLP-decarboxymyriocin aldimine **15**. Carbon atoms in protein side chains are shown as white sticks, others atoms are colored as figure 6A. The hydrocarbon chain of the myriocin inserts into a hydrophobic pocket. (D) Superposition of the PLP-decarboxymyriocin external aldimine (colored as before) with the PLP-L-serine external aldimine 2W8J (cartoon pale orange, protein side chain carbons dark grey, aldimine carbons colored green, other atoms are colored as before). The key catalytic Lys265 residue is mutated to Ala in the decarboxylated myriocin complex. (E) Decarboxylation mechanism to account for PLP-decarboxymyriocin external aldimine observed in the crystal structure of SPT K265A.

Comparison of this complex with the wild type SPT:PLP-L-serine external aldimine complex (PDB code 2W8J)[8b] reveals essentially the same positioning of the PLP rings in both structures (**Figure 6D**). Moreover, many key active site residues (His159, Asp231, His234) adopt similar positions. However Arg378, which is involved in a key electrostatic interaction with the carboxylate of L-serine in the SPT:PLP-L-serine external aldimine structure, is swung out of the active site with concomitant change in the important mobile loop 378 RPPATP 383; both the loop and Arg378 are partially disordered in the new complex. These changes are the result of accommodating the extended hydrophobic tail of **15**. We also note that Arg390, a conserved residue which is required for product formation in the SPT catalytic cycle[27], adjusts its side chain conformation and makes interactions with both Tyr73 and the C4 hydroxyl of myriocin. In the experimental maps the aromatic portion of the side chain of Tyr73 is not visible in the experimental density despite other plausible conformations being precluded by packing. We confirmed by DNA sequencing and mass spectrometry the residue was tyrosine.

Discussion

Natural products and their derivatives are responsible for over half of all Food and Drug Administration (FDA)-approved drugs[28] and continue to provide excellent lead molecules.[29] Natural products also serve as excellent chemical probes that can be used to tease out the fine details of biochemical pathways and networks.[30] Myriocin, as well as possessing potent antifungal, antibacterial and immune suppression activity, is also a valuable chemical tool. Recently Breslow *et al.* used myriocin to probe the multi-protein, membrane-bound SPT complex (denoted SPOTs) from the endoplasmic reticulum (ER) of yeast that contains SPT1, SPT2, TSC3P, ORM proteins and Sac1 phosphatase.[2c] The SPOTs complex is now known to be central to SL biosynthesis in higher organisms acting as a metabolic rheostat.[31] SLs are now recognised as important in the aetiology of many significant human diseases. The pro-drug fingolimod, 2-amino-2-[2-(4-octylphenyl)ethyl]propane-1,3-diol, becomes phosphorylated and mimics sphingosine 1-phosphate (S1P) in the body. The drug suppresses the immune system and is used in the treatment of relapsing remitting multiple sclerosis where it is thought to work by binding to S1P receptors. There is now widespread interest in regulating the production of SLs in the body and the most obvious target is the SPOTs complex which contains SPT. There are two related obstacles to progress, firstly the human SPOTs complex is not currently tractable to biochemical study and there is very limited understanding of how the exemplar inhibitor myriocin works at a molecular level. To overcome these obstacles we have employed the bacterial SPT homolog to reveal the molecular details of myriocin inhibition for the first time.

We have experimentally confirmed the existence of the previously assumed SPT:PLP-myriocin external aldimine inhibitor complex (**11**) by mass spectrometry and spectroscopy (**Figure 2B and 2C**). We observed that myriocin (K_i 967 nM) was a potent competitive inhibitor for both L-serine and palmitoyl-CoA, an observation consistent with the ordered, bi-bi mechanism of AOS enzymes and the inhibitor acting as a intermediate mimic. Despite this nanomolar potency we were unable to completely abolish the activity of the

enzyme, our data suggest that this is because at the con-centration of the enzyme required for reliable assay, we cannot dissolve sufficient myriocin to saturate the binding site. *In vivo*, with endogenous SPT levels (found within an ER-bound, SPOTs complex) where the enzyme is in a hydrophobic lipid environment, this limitation is not expected to occur. The Schiff's base external aldimine formed between PLP and myriocin (**11**) is analogous to that formed between PLP and D-serine, a known, but weak, SPT inhibitor.[32] This inhibition should be reversible by incubation with fresh PLP which would displace the inhibitor and restore the holo, internal aldimine form. Indeed, this was the case but only if the PLP was added to the enzyme:inhibitor complex relatively soon after it was formed. However, addition of PLP could not rescue the enzyme if the SPT:PLP-myriocin complex was subjected to prolonged incubation.

Coupled to this surprising result regarding the kinetics we also observed interesting, time-dependent spectroscopic changes of the SPT:PLP-myriocin external aldimine complex (**11**). This suggested to us that this initial complex was breaking down to an unanticipated second inhibitory species. We generated an inactive SPT (K265A) by removal of the key, conserved active site lysine which not only binds the PLP but also plays an essential role in acid/base catalysis during the mechanism. The SPT K265A mutant binds PLP (albeit non-covalently) and forms the PLP-myriocin external aldimine **11** but it does not undergo the apparent breakdown observed with the wild-type enzyme suggesting Lys265 is crucial for this enzyme-catalysed reaction. Mass spectrometry and chemical reduction establishes that in the wild type SPT the PLP-myriocin external aldimine converts to a C18 imine adduct of Lys265, the key catalytic residue. This covalent modification results in irreversible inhibition of SPT that cannot be rescued by incubation with PLP. This result was entirely unexpected and suggested both a previously unsuspected catalytic activity of SPT, as well as a novel duel mechanism of action of SPT inhibition by myriocin.

We were unable to obtain crystals of the wild-type enzyme with myriocin in the active site presumably because the PLP-myriocin aldimine degrades during the two week timescale of crystallisation. However, the catalytically inactive K265A mutant did allow us to capture an external aldimine complex; but even then the refined structure revealed that it had undergone a surprising decarboxylation leaving a PLP-decarboxymyriocin aldmine **15** in the active site. To investigate the time-scale of this decarboxylation process we used mass spectrometry analysis of the SPT K265A:myriocin incubation and found that the PLP-myriocin aldimine (**11**) is stable at room temperature for at least seven days with decarboxylation only observed to occur after this time (**Supplementary Figure 5**).

PLP is a versatile cofactor that can use the electron sink properties of the protonated pyridine ring to catalyse a wide range of reactions of amino acid substrates including racemisation and decarboxylation.[33] These different chemical reactions proceed from the same key, PLP-amino acid external aldimine and are controlled by the architecture of the particular enzyme active site. Dunathan put forward a hypothesis that outlined the stereo-electronic constraints that govern PLP-dependent enzymes.[34] Modelling the SPT K265A PLP-myriocin external aldimine complex (**11**) places the carboxylate perpendicular to the PLP ("Dunathan conformation")

that would allow decarboxylation by the mechanism proposed in **Figure 6E**. However, its extreme slowness relative to *bone fide* PLP-dependent decarboxylases, cautions that the PLP-myriocin aldimine in K265A is not optimally aligned for this reaction. It is worth noting here that the precise orientation of the PLP-myriocin aldimine required for decarboxylation may not be achievable to the wild type enzyme. In the wild type SPT the side chain of K265 would be very close to/clash with the carboxylate, perhaps distorting it out of the Dunathan conformation or stabilising the carboxylate by an ionic interaction. In our previous study of the SPT:PLP-L-serine external aldimine complex of S. *paucimoblis* SPT we revealed that the carboxylate group is held in a specific orientation by salt bridges with Arg378 and His159.[8b, 27] In this arrangement decarboxylation is not favoured, rather deprotonation of the L-serine at C α by K265 is achieved only upon a conformational change caused by palmitoyl-CoA binding (**Figure 1**). [8b, 35]

An overlay of the wild-type PLP-L-serine and the K265A PLP-decarboxymyriocin structures reveals that the configuration of the SPT active site remains relatively well conserved (**Figure 6D**) as well as providing a molecular insight into why myriocin is a nanomolar inhibitor (**Supplementary Figure S6a**). Conserved residues His159, Asp231 and His234 are all in the same relative positions within the active site. Moreover, the CH_2OH head group of myriocin interacts with the 5′-phosphate of PLP in the same manner as the hydroxyl group from L-serine (**Supplementary Figure S6b)**. Of key note, the 3,4 *cis* diol of decarboxymyriocin makes hydrogen bonds to the protein, notably the 3-hydroxy of myriocin with the important catalytic residue His159; this interaction would be expected to be preserved in the wild type SPT:myriocin complex. The hydrogen bond network that surrounds and includes the 4-hydroxy of decarboxymyriocin may be changed by the presence of Lys265 but at least some of the same network seems certain to persist and this too involves the same residues that interact with the carboxylate of the PLP-L-serine external aldimine. These interactions rationalise the competitive inhibition with L-serine. Accompanying these interactions are movements of the side-chains of Tyr73, Arg378 and Arg390 as well as a displacement of a key conserved stretch of amino acids (RPPATP) that constitute a mobile loop that undergoes conformational changes during the catalytic cycle. The 6,7 *trans* double bond geometry of myriocin is clearly defined and we can see electron density for the carbon chain up to C9 which sits in the hydrophobic cleft adjacent to PLP. The carbon tail of myriocin binds in a similar orientation to the decanoyl-tail of the PLP-product external aldimine observed bound in the crystal structure of the related AOS enzyme CqsA from *Vibrio cholera* (**Supplementary Figure S7)**[7] consistent with our hypothesis that myriocin mimics the condensation intermediate.

The structure also rationalises the unexpected retro-aldol degradation of the PLP-myriocin external aldimine **11** into the C18 aldehyde **12**. This mechanism requires a base to abstract the proton from the 3-hydroxy of myriocin. Based on its role in the SPT reaction and the fact that a K265A mutant was unable to catalyse the retro-aldol myriocin degradation, Lys265 was a prime candidate for this role. However, structural overlay suggests that Lys265 would be on the wrong face to perform this role **(Figure 6D)**. However, the absolutely conserved His159 is positioned 2.6 Å away from the 3-hydroxy of myriocin and we propose that it initiates the breakage of the C2-C3 bond with the electrons sinking into the PLP ring (**Figure 4** and **Supplementary**

Figure S6a). Unfortunately, it is difficult to test this hypothesis using site-directed mutagenesis at this position since Ikushiro and colleagues showed that SPT His159 mutants are catalytically compromised enzymes that favour abortive transamination of L-serine.[36] With respect to the role of Lys265 during the retro-aldol reaction, we favour a mechanism in which it protonates the resulting formal carbanion at C2, acting as an acid. This would explain why the K265A mutant does not catalyse the retro-aldol reaction. Again we caution the slowness of the reaction indicates that the enzyme is not optimally arranged for this catalysis although it does occur over a timescale that we monitored spectroscopically. Having carried out this chemistry, the deprotonated lysine is perfectly positioned to attack the newly formed C18 aldehyde species (**12**) to form a covalent aldimine adduct (**14**) (**Figure 7**). Such a hydrophobic C18 molecule would be predicted to slowly dissociate and thus favour imine formation over release from the enzyme. Since this second inhibitor modifies the key catalytic lysine residue irreversibly, it will block access to the active site and prevent regeneration by PLP on a biologically-relevant timescale. Indeed, we show that the enzyme remained inhibited by this species 72 hours after extensive dialysis. The observed stability of the long chain imine (**14**) may well be due to the presence of the alpha hydroxyl; which will allow tautomerization to the alpha-aminoketone via the amino-enolate.

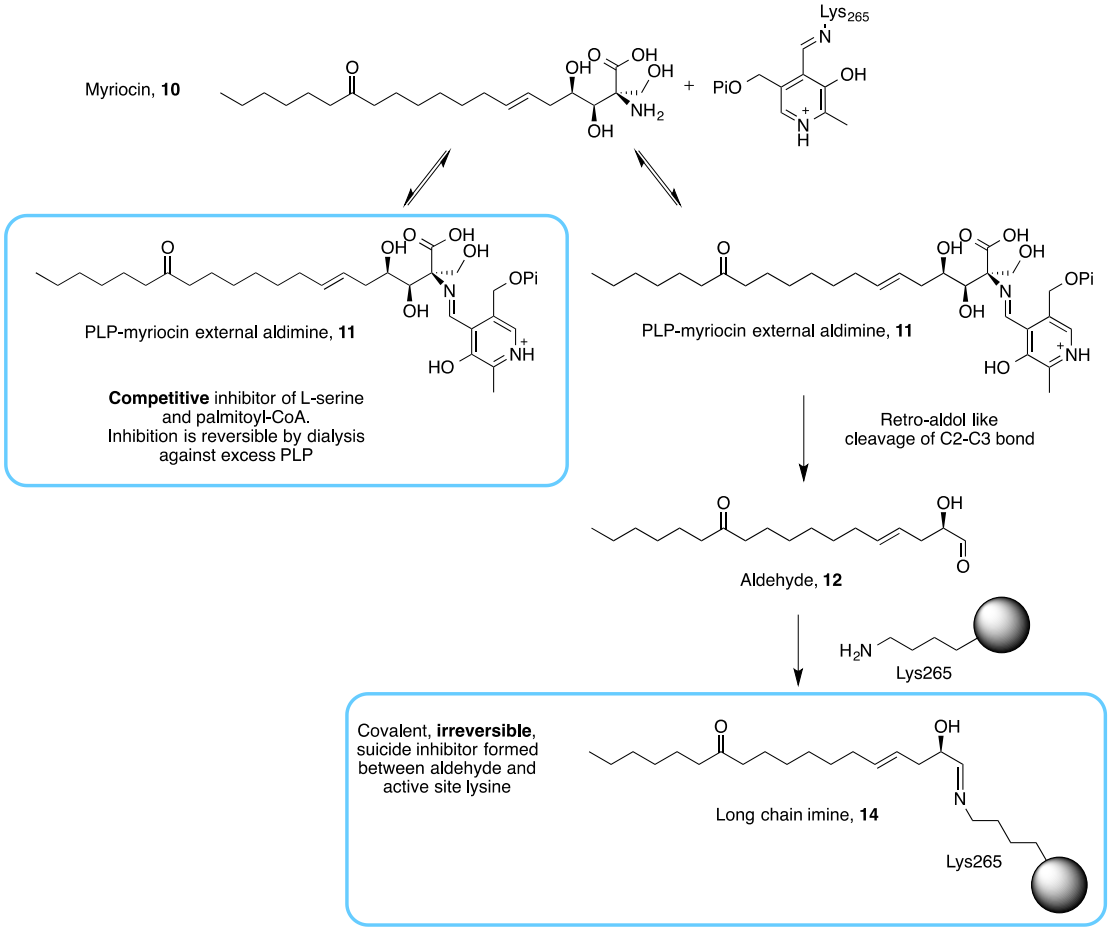

Figure 7. Summary of myriocin's dual mode of action. Inhibitory species highlighted in boxes. Left. Myriocin reacts with PLP in the active site to form the inhibitory PLP-myriocin aldimine **11**, this species is stable for

greater than an hour at physiological temperature with inhibition being reversible upon addition of excess PLP. Right. PLP-myriocin aldimine **11** decomposes over 16 hours, at physiological temperature, to produce a long chain aldehyde (**12**) that react with the active site lysine to form an imine, thus rendering the enzyme inactive. This covalent modification can be classed as suicide inhibition.

Conclusion

We set out to delineate the structural and mechanistic details of how myriocin inhibits SPT and in doing so we have revealed unexpected and hitherto unprecedented chemistry (summarised in **Figure 7**). Our results demonstrate that, as predicted, myriocin acts as a classical intermediate mimic inhibitor with nanomolar affinity for its target. However, once bound in the active site the inhibitory species is broken down by the enzyme to generate a reactive product which acts a suicide inhibitor by covalent modification of a key active site residue conserved in all SPTs.

The PLP-catalysed retro-aldol reaction that breaks down the myriocin calls to mind other important PLP-dependent enzymes that use the cofactor to catalyse C-C bond cleavage. Serine hydroxymethyltransferase[37], which is involved in one carbon metabolism; and CqsA[7], which produces quorum sensing molecules, both use a proposed retro-aldol mechanism to generate glycine from L-serine and L-threonine respectively. Furthermore, the proposed mechanism for myriocin degradation is reminiscent of the mechanism of the PLP-dependent sphingosine-1-phosphate (S1P) lyase (S1PL), the terminal enzyme of SL biosynthesis that catalyses the breakdown of S1P.[38] During the catalytic cycle of S1PL, the C3 hydroxyl group of the key PLP-S1P external aldimine is deprotonated, which leads to C2-C3 bond cleavage and production of hexadecenal and phosphoethanolamine. The similarity of the long chain aldehyde product of S1PL to the suicide-inhibitor produced by SPT-catalysed breakdown of myriocin, **12**, is striking. This suggested to us a possible feedback mechanism whereby the end product of the SL pathway, hexadecenal, may regulate SL biosynthesis by inhibiting SPT, the enzyme that catalyses the first step in de novo SL synthesis. Indeed, in preliminary *in vitro* studies, we have found that hexadecanal inhibits SPT with an IC_{50} of 144 μM (**Supplementary Figure S8).**

The high sequence homology between the SPTs from bacteria and other higher order species suggest that the mechanism of myriocin inhibition is conserved, and studies on the human enzyme are underway. The unprecedented combination of tight binding and mechanism-based inactivation within a single molecule described herein has the potential to inform the design of a new class of inhibitors for SPT and other PLP-dependent enzymes.

Notes and references

[1] (a) Pruett, S. T.; Bushnev, A.; Hagedorn, K.; Adiga, M.; Haynes, C. A.; Sullards, M. C.; Liotta, D. C.; Merrill, A. H., Thematic Review Series: Sphingolipids. Biodiversity of sphingoid bases "sphingosines" and related amino alcohols. *J. Lipid Res.* **2008,** *49* (8), 1621-1639; (b) Merrill, A. H., Sphingolipid and Glycosphingolipid Metabolic Pathways in the era of Sphingolipidomics. *Chem. Rev.* **2011,** *111* (10), 6387-6422.

[2] (a) Summers, S. A.; Nelson, D. H., A Role for Sphingolipids in Producing the Common Features of Type 2 Diabetes, Metabolic Syndrome X, and Cushing's Syndrome. *Diabetes* **2005,** *54* (3), 591-602; (b) van Echten-Deckert, G.; Walter, J., Sphingolipids: Critical players in Alzheimer's disease. *Prog. Lipid Res.* **2012,** *51* (4), 378-393; (c) Breslow, D. K.; Collins, S. R.; Bodenmiller, B.; Aebersold, R.; Simons, K.; Shevchenko, A.; Ejsing, C. S.; Weissman, J. S., Orm family proteins mediate sphingolipid homeostasis. *Nature* **2010,** *463* (7284), 1048-1053.

[3] Yeung, B. K. S., Natural product drug discovery: the successful optimization of ISP-1 and halichondrin B. *Curr. Opin. Chem. Biol.* **2011,** *15* (4), 523-528.

[4] Webster, S. P.; Alexeev, D.; Campopiano, D. J.; Watt, R. M.; Alexeeva, M.; Sawyer, L.; Baxter, R. L., Mechanism of 8-Amino-7-oxononanoate Synthase: Spectroscopic, Kinetic, and Crystallographic Studies†,‡. *Biochemistry* **2000,** *39* (3), 516-528.

[5] Schmidt, A.; Sivaraman, J.; Li, Y.; Larocque, R.; Barbosa, J. A. R. G.; Smith, C.; Matte, A.; Schrag, J. D.; Cygler, M., Three-Dimensional Structure of 2-Amino-3-ketobutyrate CoA Ligase from Escherichia coli Complexed with a PLP−Substrate Intermediate: Inferred Reaction Mechanism. *Biochemistry* **2001,** *40* (17), 5151-5160.

[6] Astner, I.; Schulze, J. O.; van den Heuvel, J.; Jahn, D.; Schubert, W.-D.; Heinz, D. W., Crystal structure of 5-aminolevulinate synthase, the first enzyme of heme biosynthesis, and its link to XLSA in humans. *EMBO J.* **2005,** *24* (18), 3166-3177.

[7] Jahan, N.; Potter, J. A.; Sheikh, M. A.; Botting, C. H.; Shirran, S. L.; Westwood, N. J.; Taylor, G. L., Insights into the Biosynthesis of the Vibrio cholerae Major Autoinducer CAI-1 from the Crystal Structure of the PLP-Dependent Enzyme CqsA. *J. Mol. Biol.* **2009,** *392* (3), 763-773.

[8] (a) Yard, B. A.; Carter, L. G.; Johnson, K. A.; Overton, I. M.; Dorward, M.; Liu, H.; McMahon, S. A.; Oke, M.; Puech, D.; Barton, G. J.; Naismith, J. H.; Campopiano, D. J., The Structure of Serine Palmitoyltransferase; Gateway to Sphingolipid Biosynthesis. *J. Mol. Biol.* **2007,** *370* (5), 870-886; (b) Raman, M. C. C.; Johnson, K. A.; Yard, B. A.; Lowther, J.; Carter, L. G.; Naismith, J. H.; Campopiano, D.

J., The External Aldimine Form of Serine Palmitoyltransferase. *J. Biol. Chem.* **2009,** *284* (25), 17328-17339.

[9] Raboni, S.; Spyrakis, F.; Campanini, B.; Amadasi, A.; Bettati, S.; Peracchi, A.; Mozzarelli, A.; Contestabile, R.; Lew, M.; Hung-Wen, L., Pyridoxal 5'-Phosphate-Dependent Enzymes: Catalysis, Conformation, and Genomics. In *Comprehensive Natural Products II*, Elsevier: Oxford, 2010; pp 273-350.

[10] (a) Lowther, J.; Yard, B. A.; Johnson, K. A.; Carter, L. G.; Bhat, V. T.; Raman, M. C. C.; Clarke, D. J.; Ramakers, B.; McMahon, S. A.; Naismith, J. H.; Campopiano, D. J., Inhibition of the PLP-dependent enzyme serine palmitoyltransferase by cycloserine: evidence for a novel decarboxylative mechanism of inactivation. *Molecular BioSystems* **2010,** *6* (9), 1682-1693; (b) Lowther, J.; Beattie, A. E.; Langridge-Smith, P. R. R.; Clarke, D. J.; Campopiano, D. J., L-Penicillamine is a mechanism-based inhibitor of serine palmitoyltransferase by forming a pyridoxal-5'-phosphate-thiazolidine adduct. *MedChemComm* **2012,** *3* (8), 1003-1008; (c) Badet, B.; Roise, D.; Walsh, C. T., Inactivation of the dadB Salmonella typhimurium alanine racemase by D and L isomers of beta-substituted alanines: kinetics, stoichiometry, active site peptide sequencing, and reaction mechanism. *Biochemistry* **1984,** *23* (22), 5188-94.

[11] (a) Conti, P.; Tamborini, L.; Pinto, A.; Blondel, A.; Minoprio, P.; Mozzarelli, A.; De Micheli, C., Drug Discovery Targeting Amino Acid Racemases. *Chem. Rev.* **2011,** *111* (11), 6919-6946; (b) Amadasi, A.; Bertoldi, M.; Contestabile, R.; Bettati, S.; Cellini, B.; di Salvo, M. L.; Borri-Voltattorni, C.; Bossa, F.; Mozzarelli, A., Pyridoxal 5'-phosphate enzymes as targets for therapeutic agents. *Curr Med Chem* **2007,** *14* (12), 1291-324.

[12] (a) Fujita, T.; Hirose, R.; Yoneta, M.; Sasaki, S.; Inoue, K.; Kiuchi, M.; Hirase, S.; Chiba, K.; Sakamoto, H.; Arita, M., Potent Immunosuppressants, 2-Alkyl-2-aminopropane-1,3-diols1. *J. Med. Chem.* **1996,** *39* (22), 4451-4459; (b) Ikushiro, H.; Hayashi, H.; Kagamiyama, H., Reactions of Serine Palmitoyltransferase with Serine and Molecular Mechanisms of the Actions of Serine Derivatives as Inhibitors *Biochemistry* **2004,** *43* (4), 1082-1092; (c) Hanada, K.; Nishijima, M.; Fujita, T.; Kobayashi, S., Specificity of inhibitors of serine palmitoyltransferase (SPT), a key enzyme in sphingolipid biosynthesis, in intact cells: A novel evaluation system using an SPT-defective mammalian cell mutant. *Biochem. Pharmacol.* **2000,** *59* (10), 1211-1216; (d) Miyake, Y.; Kozutsumi, Y.; Nakamura, S.; Fujita, T.; Kawasaki, T., Serine Palmitoyltransferase Is the Primary Target of a Sphingosine-like Immunosuppressant, ISP-1/Myriocin. *Biochem. Biophys. Res. Commun.* **1995,** *211* (2), 396-403.

[13] (a) Kluepfel, D.; Bagli, J.; Baker, H.; Charest, M. P.; Kudelski, A., Myriocin, a new antifungal antibiotic from Myriococcum albomyces. *J Antibiot (Tokyo)* **1972,** *25* (2), 109-15; (b) Aragozzini, F.; Manachini, P. L.; Craveri, R.; Rindone, B.; Scolastico, C., Isolation and structure determination of a new antifungal α-hydroxymethyl-α-amino acid. *Tetrahedron* **1972,** *28* (21), 5493-5498.

[14] Fujita, T.; Inoue, K.; Yamamoto, S.; Ikumoto, T.; Sasaki, S.; Toyama, R.; Chiba, K.; Hoshino, Y.; Okumoto, T., Fungal metabolites. Part 11. A potent immunosuppressive activity found in Isaria sinclairii metabolite. *J Antibiot (Tokyo)* **1994,** *47* (2), 208-15.

[15] Chen, J. K.; Lane, W. S.; Schreiber, S. L., The identification of myriocin-binding proteins. *Chemistry & Biology* **1999,** *6* (4), 221-235.

[16] Han, S.; Lone, M. A.; Schneiter, R.; Chang, A., Orm1 and Orm2 are conserved endoplasmic reticulum membrane proteins regulating lipid homeostasis and protein quality control. *Proceedings of the National Academy of Sciences* **2010,** *107* (13), 5851-5856.

[17] Liu, H.; Naismith, J., An efficient one-step site-directed deletion, insertion, single and multiple-site plasmid mutagenesis protocol. *BMC Biotechnology* **2008,** *8* (1), 1-10.

[18] Williams, J. W.; Morrison, J. F., [17] The kinetics of reversible tight-binding inhibition. In *Methods Enzymol.*, Daniel, L. P., Ed. Academic Press: 1979; Vol. Volume 63, pp 437-467.

[19] (a) Cha, S., Tight-binding inhibitors: Kinetic behavior. *Biochem. Pharmacol.* **1975,** *24* (23), 2177-2185; (b) Williams, J.; Morrison, J., The kinetics of reversible tight-binding inhibition. *Methods Enzymol* **1979,** *63*, 437-467.

[20] Winter, G., xia2: an expert system for macromolecular crystallography data reduction. *J. Appl. Crystallogr.* **2010,** *43* (1), 186-190.

[21] McCoy, A. J.; Grosse-Kunstleve, R. W.; Adams, P. D.; Winn, M. D.; Storoni, L. C.; Read, R. J., Phaser crystallographic software. *J. Appl. Crystallogr.* **2007,** *40* (Pt 4), 658-674.

[22] Schuttelkopf, A. W.; van Aalten, D. M. F., PRODRG: a tool for high-throughput crystallography of protein-ligand complexes. *Acta Crystallographica Section D* **2004,** *60* (8), 1355-1363.

[23] Winn, M. D.; Isupov, M. N.; Murshudov, G. N., Use of TLS parameters to model anisotropic displacements in macromolecular refinement. *Acta Crystall D Biol Crystallogr* **2001,** *57* (pt 1), 122-33.

[24] Emsley, P.; Cowtan, K., Coot: model-building tools for molecular graphics. *Acta Crystallogr D Biol Crystallogr* **2004,** *60* (Pt 12 Pt 1), 2126-32.

[25] Davis, I. W.; Leaver-Fay, A.; Chen, V. B.; Block, J. N.; Kapral, G. J.; Wang, X.; Murray, L. W.; Arendall, W. B., 3rd; Snoeyink, J.; Richardson, J. S.; Richardson, D. C., MolProbity: all-atom contacts and structure validation for proteins and nucleic acids. *Nucleic Acids Res.* **2007,** *35* (Web Server issue), W375-83.

[26] Hanada, K., Serine palmitoyltransferase, a key enzyme of sphingolipid metabolism. *Biochimica et Biophysica Acta (BBA) - Molecular and Cell Biology of Lipids* **2003,** *1632* (1-3), 16-30.

[27] Lowther, J.; Charmier, G.; Raman, M. C.; Ikushiro, H.; Hayashi, H.; Campopiano, D. J., Role of a conserved arginine residue during catalysis in serine palmitoyltransferase. *FEBS Lett.* **2011,** *585* (12), 1729-1734.

[28] (a) Newman, D. J.; Cragg, G. M., Natural products as sources of new drugs over the 30 years from 1981 to 2010. *J Nat Prod* **2012,** *75* (3), 311-35; (b) Swinney, D.; Anthony, J., How were new medicines discovered? *Nature Reviews Drug Discovery* **2011,** *10*, 507-519; (c) Schulze, C. J.; Bray, W. M.; Woerhmann, M. H.; Stuart, J.; Lokey, R. S.; Linington, R. G., "Function-first" lead discovery: mode of action profiling of natural product libraries using image-based screening. *Chem Biol* **2013,** *20* (2), 285-95.

[29] (a) Jesse, W.-H. L.; Vederas, J. C., Drug Discovery and Natural Products: End of an Era or an Endless Frontier? *Science* **2009,** *325* (5937), 161-165; (b) Fischbach, M. A.; Walsh, C. T., Antibiotics for Emerging Pathogens. *Science* **2009,** *325* (5944), 1089-1093.

[30] Carlson, E. E., Natural Products as Chemical Probes. *ACS Chemical Biology* **2010,** *5* (7), 639-653.

[31] Tafesse, F. G.; Holthuis, J. C. M., Cell biology: A brake on lipid synthesis. *Nature* **2010,** *463* (7284), 1028-1029.

[32] Hanada, K.; Hara, T.; Nishijima, M., D-Serine inhibits serine palmitoyltransferase, the enzyme catalyzing the initial step of sphingolipid biosynthesis. *FEBS Lett.* **2000,** *474* (1), 63-65.

[33] Eliot, A. C.; Kirsch, J. F., PYRIDOXAL PHOSPHATE ENZYMES: Mechanistic, Structural, and Evolutionary Considerations. *Annu. Rev. Biochem* **2004,** *73* (1), 383-415.

[34] Dunathan, H. C., Conformation and reaction specificity in pyridoxal phosphate enzymes. *Proceedings of the National Academy of Sciences of the United States of America* **1966,** *55* (4), 712-716.

[35] Ikushiro, H.; Fujii, S.; Shiraiwa, Y.; Hayashi, H., Acceleration of the Substrate Cα Deprotonation by an Analogue of the Second Substrate Palmitoyl-CoA in Serine Palmitoyltransferase. *J. Biol. Chem.* **2008,** *283* (12), 7542-7553.

[36] Shiraiwa, Y.; Ikushiro, H.; Hayashi, H., Multifunctional Role of His159in the Catalytic Reaction of Serine Palmitoyltransferase. *J. Biol. Chem.* **2009,** *284* (23), 15487-15495.

[37] Florio, R.; di Salvo, M. L.; Vivoli, M.; Contestabile, R., Serine hydroxymethyltransferase: A model enzyme for mechanistic, structural, and evolutionary studies. *Biochimica et Biophysica Acta (BBA) - Proteins and Proteomics* **2011,** *1814* (11), 1489-1496.

[38] 38.Bourquin, F.; Capitani, G.; Grutter, M. G., PLP-dependent enzymes as entry and exit gates of sphingolipid metabolism. *Protein Sci* **2011,** *20* (9), 1492-508.